

## A Visual Description of the Convective Flow Field around the Head of a Human

Özcan, O.\*<sup>1</sup>, Meyer, K. E.\*<sup>2</sup> and Melikov, A. K.\*<sup>2</sup>

\*1 Faculty of Mechanical Engineering, Yıldız Technical University, Istanbul 34349, Turkey.  
E-mail: oktayo@yildiz.edu.tr

\*2 International Centre for Indoor Environment and Energy, Department of Mechanical Engineering,  
Technical University of Denmark, DK-2800, Lyngby, Denmark.

Received 24 July 2003  
Revised 6 June 2004

**Abstract:** Mean velocity data obtained by PIV (Particle Image Velocimetry) around the head of a real-life size breathing thermal manikin are presented for two cases of 'no breathing' and 'continuous exhalation through nose'. Experiments were conducted in a special chamber which provided stationary convective flows around the seated manikin. Results are limited to the plane of symmetry. The paper aims to describe the physical structure of the turbulent flow field by presenting velocity and vorticity data in color graphics.

**Keywords:** PIV, Turbulence, Free and Forced Convection, Streamline Topology.

### 1. Introduction

Approximately 35 % of metabolic heat from a human body is dissipated by convective means as reported by Homma and Yakiyama (1987). The resulting flow field is of significant interest due to its relevance to ventilation, heating and air conditioning applications in homes, offices and vehicles. The free convective flow field around a human body has been studied by Homma and Yakiyama (1987), Fiedorowicz (1972), Melikov and Zhou (1996) and Murakami, Kato and Zeng (1997).

Despite its importance and continual presence around us, little is known about the convective flow field around a human head. Lack of data is mainly due to experimental difficulties stemming from large turbulence levels and long integral time scales of the flow, and computational difficulties arising from unavailability of dependable turbulence models. PIV is capable of making accurate measurements in highly turbulent flows in a reasonably short time period. The present paper discusses flow field data obtained by PIV around the head of a real-life size breathing thermal manikin for two cases of 'no breathing' and 'continuous exhalation through nose'. Results are limited to the plane of symmetry and will be discussed in terms of mean velocity components, speed and vorticity. Turbulence quantities are discussed in a separate paper (Özcan, Meyer and Melikov, 2003).

### 2. Experimental Setup and Conditions

The experiments were conducted in a test chamber specially built for this study at the Department

of Mechanical Engineering of the Technical University of Denmark. Figure 1 gives a schematic description of the test chamber, which had a floor area of  $2.95 \times 2.95 \text{ m}^2$  and a height of 2.4 m, together with the seated manikin (1) and the PIV system (2 to 6) employed in the experiments.

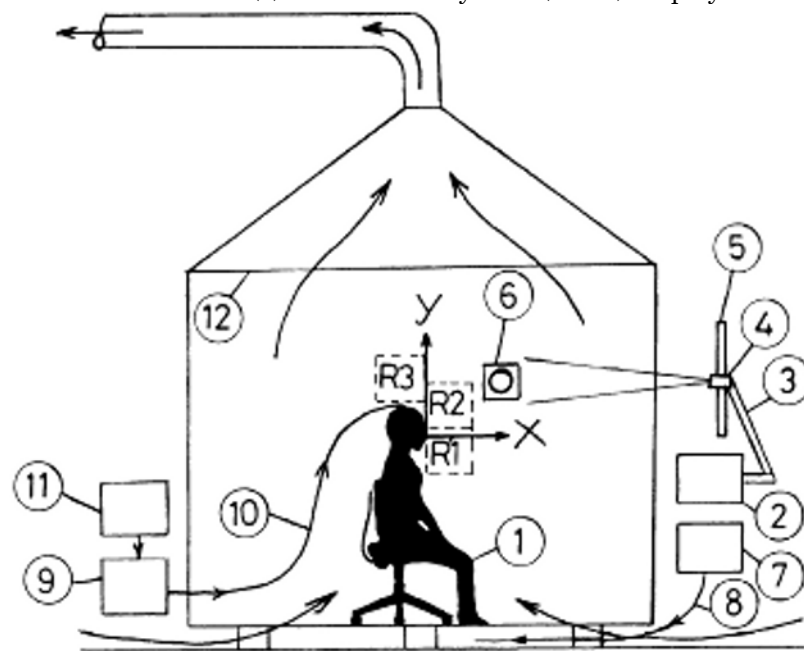


Fig. 1. Schematic drawing of test chamber (1: Manikin, 2: Laser, 3: Light guiding arm, 4: Light sheet forming optics, 5: Traverse mechanism, 6: PIV camera, 7 and 11: Seed generators, 8 and 10: Air hoses, 9: Mechanical lung, 12: Cloth screen).

Figure 1 shows the right-handed ( $x, y, z$ ) Cartesian coordinate system chosen for presentation of data.  $z$  direction is normal to the plane of the figure. The origin is located at the tip of the nose. The height of the seated manikin was 1.4 m whereas the linear room dimensions in the  $x$  and  $y$  dimensions were 2.95 m and 2.40 m, respectively. The floor was made up of steel grates with a grid size of  $0.03 \times 0.03 \text{ m}^2$  and perforated plywood plates with circular holes of  $3 \times 10^{-3} \text{ m}$  in diameter. The room air was ventilated by a variable-speed fan through a 0.3 m diameter duct connected to the roof and exhausting into atmosphere. This arrangement removed the metabolic heat generated by the manikin and hence provided a stationary thermal field, and also allowed introduction of seed particles into the chamber which was needed for PIV measurements. An orifice plate was used to measure the ventilation rate, which produced an average vertical speed of  $9 \times 10^{-3} \text{ m/s}$  in the room. A cloth screen (12) was placed at the intersection level of the roof with the side-walls in order to improve uniformity of the ventilation flow. Duct tape was used to seal the intersecting side walls and the roof-wall junctions such that there was negligibly small airflow through the walls. 20 thermistors were placed on the side-walls and the floor to monitor and record room temperature which could be considered as constant at  $T_r = 19.9 \text{ }^\circ\text{C}$  within  $0.6 \text{ }^\circ\text{C}$  during experiments.

The breathing thermal manikin used in the study was developed from a show-room display manikin and was capable of breathing through nose and/or mouth at prescribed rates and intervals. The manikin is described in detail by Melikov et al. (2000). The manikin's body was divided into 16 segments each supplied with its own measurement and control system. The comfort equation of Fanger (1970) which states a relation between heat flux from body parts ( $q$ ) and skin temperature ( $T_s$ ), was employed to prescribe the heat loss from the manikin.  $q$  varied between 76 and  $105 \text{ W/m}^2$  whereas  $T_s$  varied from 30.7 to  $32.3 \text{ }^\circ\text{C}$  over the body. Data were obtained for the nude and bald manikin who was seated upright in the center of the chamber on a frame chair facing the glass

window. Total heat loss from the manikin, total surface area and area-weighted skin temperature of the manikin ( $T_{as}$ ) were approximately 141 W, 1.48 m<sup>2</sup> and 31.3 °C, respectively. The Rayleigh number based on the height of the seated manikin (1.4 m) and the difference between the area-weighted skin temperature and room temperature ( $T_{as}-T_r$ ) was  $3.2 \times 10^9$ . The manikin is equipped with an artificial lung, which allows for adjustment of breathing mode (inhalation, exhalation), breathing frequency, respiration volumetric rate and temperature, humidity and gas composition of the exhaled air.

Data were obtained for two cases of i) 'no breathing' (free convective flow) and ii) 'continuous exhalation' (through nose at a volumetric flow rate of  $2.4 \times 10^{-4}$  m<sup>3</sup>/s). A seed generator (7) was

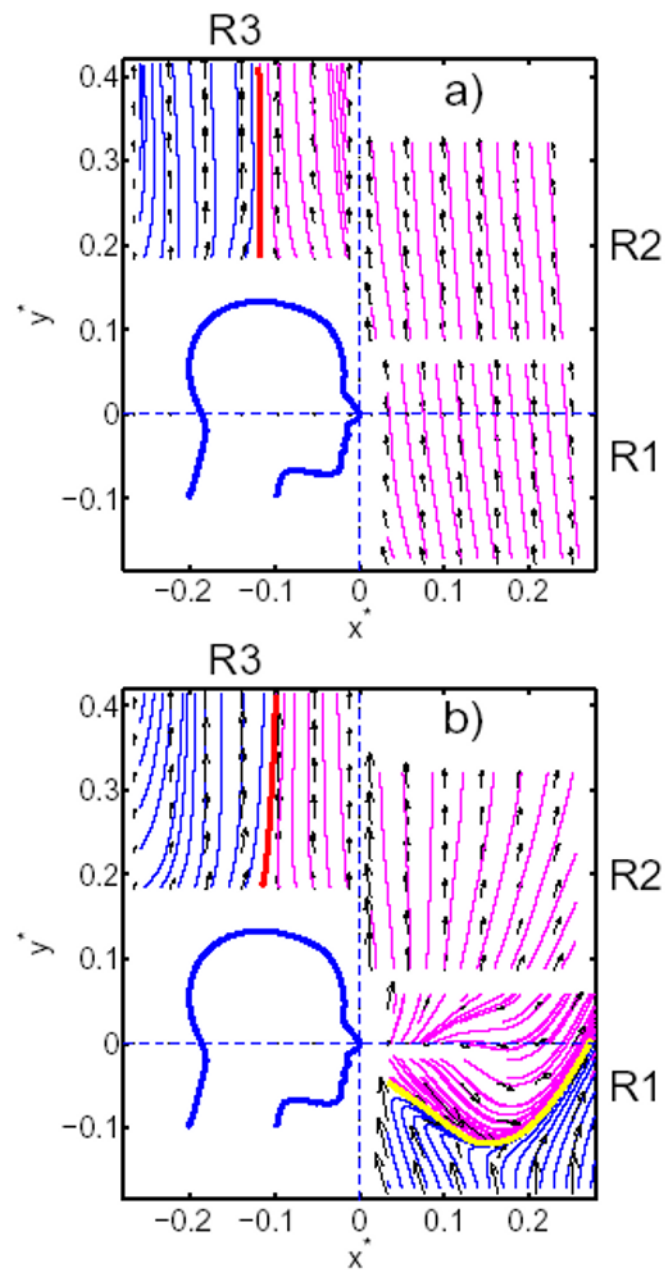


Fig. 2. Mean streamlines and (U, V) vector plots.

used to atomize and introduce Glycerine droplets of approximately  $3 \times 10^{-6}$  m in diameter into the chamber through a hose (8) extending from the generator to the bottom of the room. A second seed

generator (11) was used to seed the exhalation air for the 'continuous exhalation' case. A 'mechanical lung' (9) heated and humidified breathing air which was pumped through a hose (10) to the head of the manikin where it left nose at a temperature of 36.7 °C and a relative humidity of 95 %. A venturi meter attached to air hose (10) was used to calibrate the volumetric flow rate indicator of the mechanical lung. Inclination angles of the exhalation jet were nominally 45° and 15° relative to the x and z directions, respectively (Hyldgaard, 1994).

The value of the volumetric flow rate was chosen on the basis of information given by Åstrand and Rodahl (1970) who state that the respiration rate is approximately  $1 \times 10^{-4} \text{ m}^3/\text{s}$  for an average person (aged between 20 to 60 years) performing office work. However, the respiration cycle lasts roughly 6 s and consists of inhalation (2.5 s), exhalation (2.5 s) and break (1.0 s). Thus, for exhalation only, the flow rate is approximately  $2.4 \times 10^{-4} \text{ m}^3/\text{s}$ .

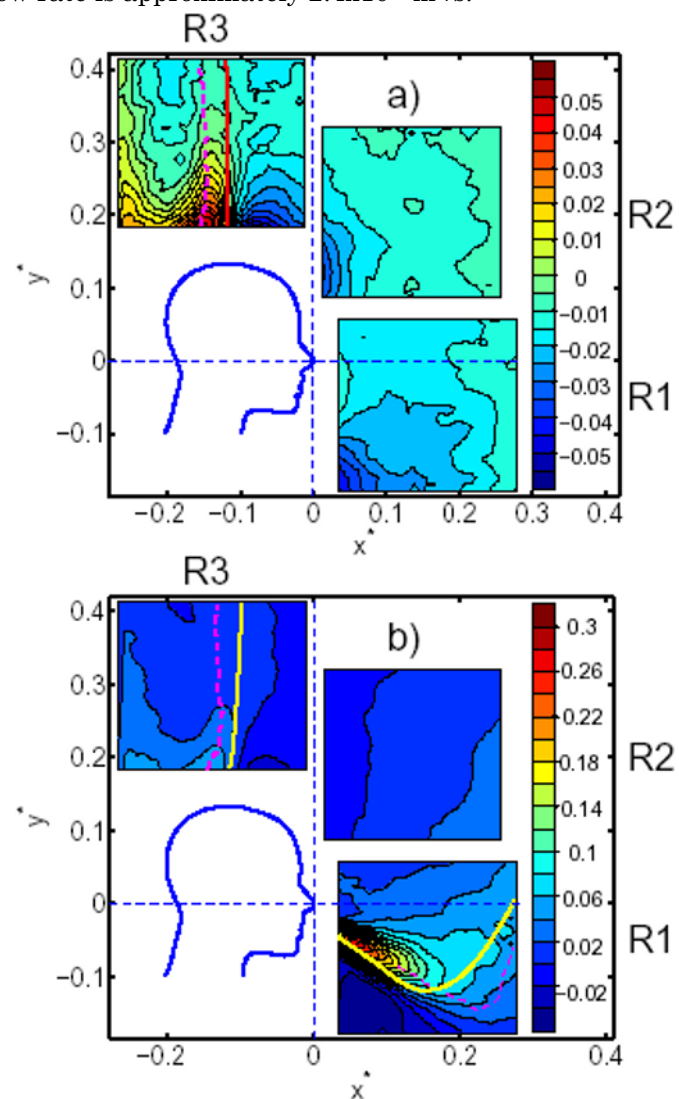


Fig. 3. Contour plots of horizontal mean velocity  $U^* = U/U_c$ . a) No breathing, b) Continuous exhalation.

Velocity data were acquired by a digital PIV system which employed a laser light sheet generated by a double cavity Nd-YAG laser (item 2 in Fig. 1) delivering up to 0.1 J light pulses. A light guiding arm (3) was employed to connect the laser with the light sheet forming optics (4) which was mounted on a traverse mechanism (5) placed outside the chamber. A Kodak Megaplug ES 1.0 camera (6) fitted with a  $532 \times 10^{-9} \text{ m}$  narrow band filter was used for recording PIV images. The laser sheet, which was approximately  $2 \times 10^{-3} \text{ m}$  in thickness, was placed in the symmetry plane

( $z=0$ ) of manikin's head. The field of view of the camera was approximately  $0.25 \times 0.25 \text{ m}^2$ . Data were obtained in regions R1, R2 and R3 which are shown in Fig. 1. R1 is the 'breathing zone' whereas R2 and R3 are the 'top of breathing zone' and the 'top of head' regions, respectively. The PIV system was controlled by a Dantec PIV2100 processor and the data were processed with Dantec Flowmanager. Adaptive correlation with moving average validation in iteration steps was employed. No filtering was used. The data was processed in 32 by 32 pixel interrogation areas with no overlap which was chosen to insure independent velocity samples. Vector maps contained  $31 \times 31$  vectors. Accurate data could not be obtained near the head due to reflections of the laser light. Some degree of deterioration in signal quality was also evident at the edges of the field of view due to decreased

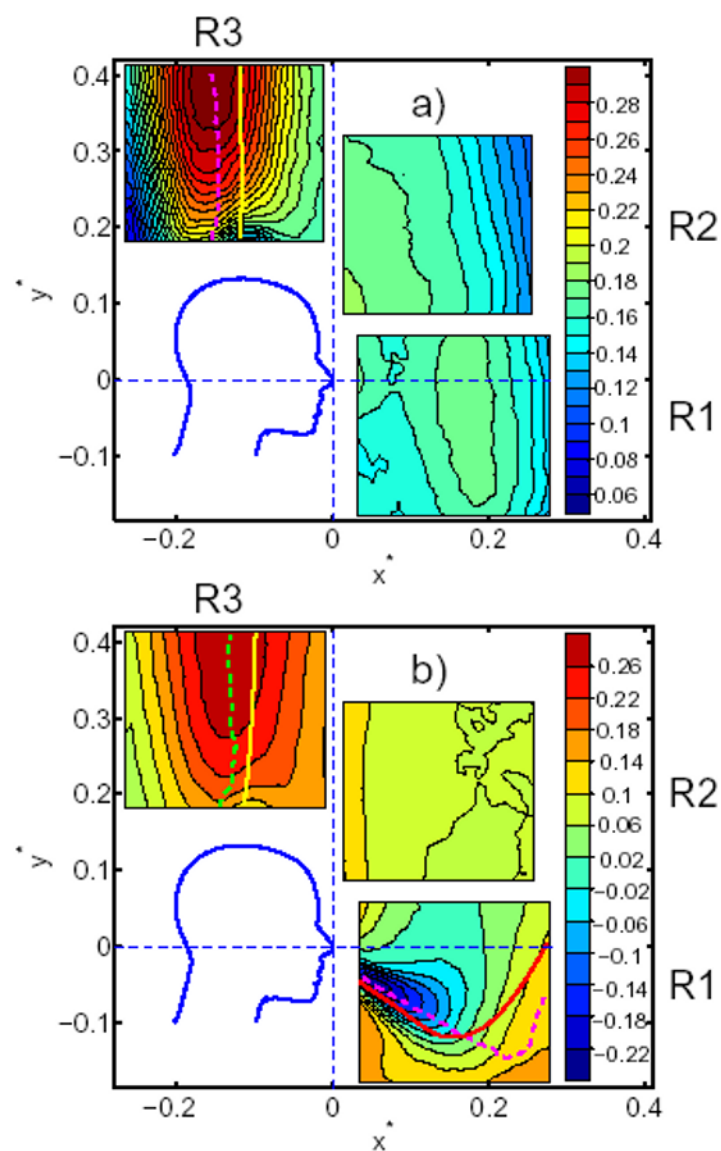


Fig. 4. Contour plots of vertical mean velocity  $V^* = V/U_c$  (a) No breathing, (b) Continuous exhalation.

intensity of the laser light. Therefore, data near the edges of the measurement area were not shown in the figures presenting the results. Image maps in all regions were recorded with a low data acquisition rate of 1 Hz which was required to attain statistical independence of velocity moments in this low speed flow. 500 instantaneous vector maps were used to calculate the mean velocity components ( $U, V$ ).

### 3. Results and Discussion

Since the manikin used in the study has real-life dimensions and heat transfer characteristics, it is practical to present the experimental data in dimensional form. Equivalently, a characteristic length scale of  $L_c=1$  m and a characteristic velocity scale of  $U_c=1$  m/s may be chosen in presenting dimensionless data. Figure 2 presents mean streamlines and  $(U, V)$  vector maps in the plane of symmetry ( $z = 0$ ) for R1, R2 and R3. Parts (a) and (b) refer to the 'no breathing' and 'continuous exhalation' cases, respectively.  $x^*$  and  $y^*$  are the normalized space variables given by  $x/L_c$  and  $y/L_c$ , respectively. Different scale factors are used in R1, R2 and R3 for vector lengths. The streamlines

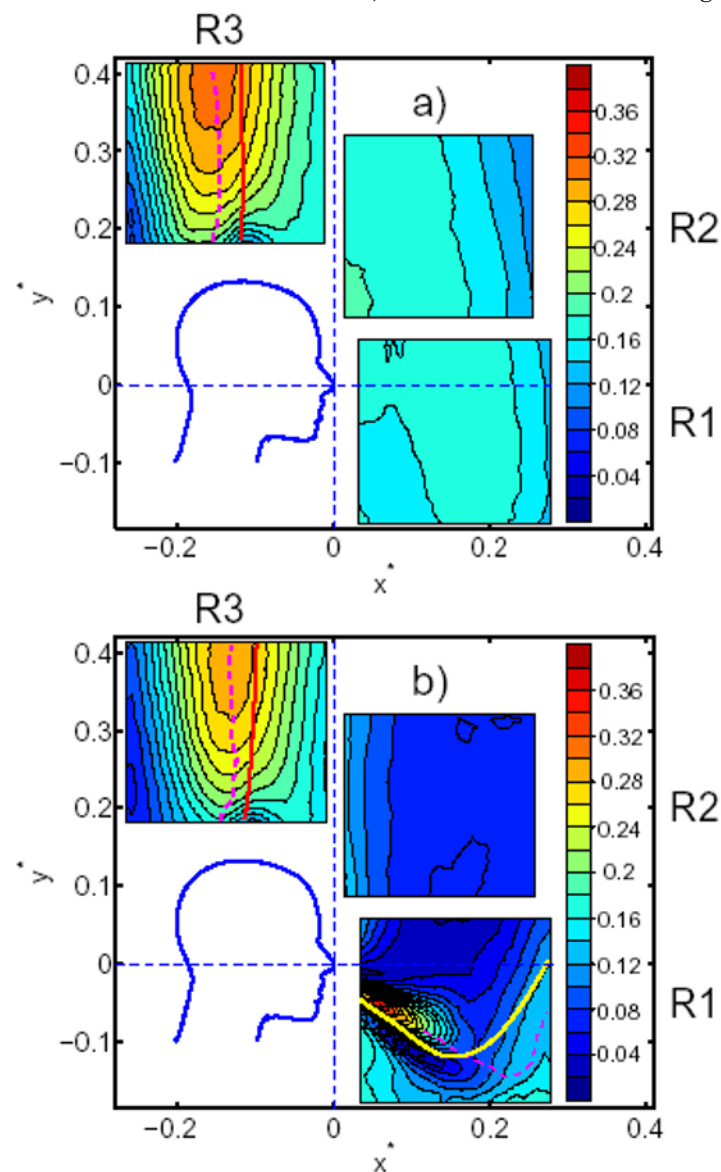


Fig. 5. Contour plots of mean speed  $Q^*=Q/U_c$  a) No breathing, b) Continuous exhalation.

and sectional streamlines are identical in this plane having zero out-of-plane velocity ( $W=0$  except for singular points). The thick continuous lines indicate dividing streamlines which have the properties of i) originating from singular points and ii) being lines of convergence for neighboring streamlines. The critical point theory outlined by Tobak and Peake (1982) and Chong and Perry (1990) states that sectional streamlines have properties consistent with those of continuous vector fields and can have a restricted number of singular (critical) points. Slope of a streamline is

indeterminate and the in-plane velocity is zero at the singular points which are classified as nodes, saddles and foci. Existence of singular points on the indicated dividing streamlines is postulated. The dividing streamline in R3 separates streamlines originating from front and back of the head. The dividing streamline in R1 for the 'continuous exhalation' case is the boundary between streamlines originating from above and below the breathing zone. Figure 2 (a) shows that all streamlines in R1 and R2 are inclined towards the face for 'no breathing' case. In contrast, for 'continuous exhalation' case, streamlines sufficiently far from the head are inclined away from the face. The dividing streamline in R3, which is almost vertical for the 'no breathing' case (Fig. 2(a)), tilts towards the breathing zone for 'continuous exhalation' (Fig. 2(b)). For the latter case, Fig.2(b) also shows that the dividing streamline close to the nose is nearly straight and inclined at  $38^\circ$  (somewhat less than the nominal inclination angle of the jet) with respect to the x axis.

Figures 3, 4 and 5 present contour plots of the normalized mean velocity components  $U^*=U/U_c$ ,  $V^*=V/U_c$  and the normalized speed  $Q^*=(U^2+V^2+W^2)^{0.5}/U_c$ , respectively, in the plane of symmetry ( $z=W=0$ ) for R1, R2 and R3. As in Fig. 2, parts (a) and (b) refer to the 'no breathing' and 'continuous exhalation' cases, respectively. Relative uncertainties in  $U^*$ ,  $V^*$  and  $Q^*$  are estimated as 7, 7 and 10 %, respectively. The thick continuous and dashed lines in R1 and R3 indicate dividing streamlines and zero vorticity lines, respectively. (Line colors may vary in Figs. 3 to 6). Comparison of Figs. 3(a) and 3(b) shows that 'continuous exhalation' eliminates the large negative  $U^*$  region

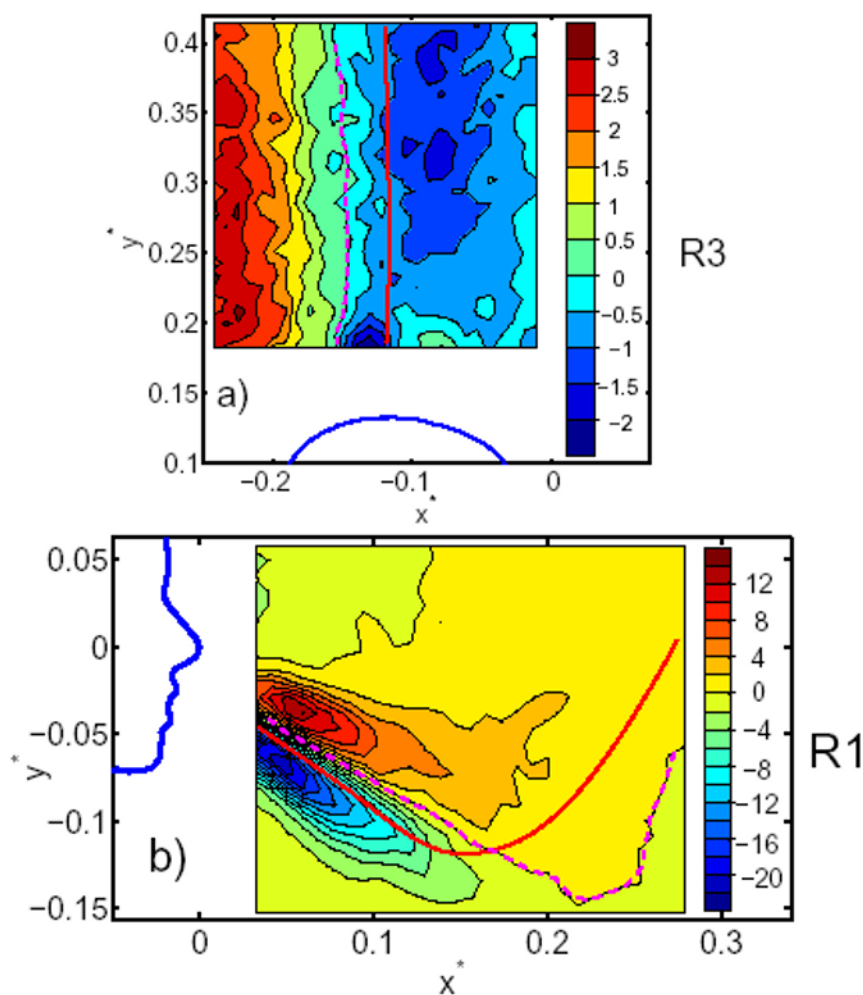


Fig. 6. Contour plots of mean vorticity  $\zeta_z^*$  a) No breathing, b) Continuous exhalation.

observed for 'no breathing' case above the head. Figures 4(a) and 5(a) show that vertical velocity  $V^*$  and speed  $Q^*$  are significantly large and nonuniform in R3 for 'no breathing' case. In contrast, Fig.

4(b) shows that for the 'continuous exhalation' case vertical velocities are relatively uniform and low in R3. It appears that rise of the thermal plume from the lap of the manikin is interrupted by the exhalation jet which generates a uniform and low vertical velocity wake in R2 and R3.

Comparison of Figs. 4(a) and 4(b) may give the false impression that vertical velocity values above the head (in R3) are significantly different for the 'no breathing' and 'continuous exhalation' cases. This is due to use of different velocity scales in Figs. 4(a) and 4(b). Line plots of  $V^*$  in R3 (not shown) indicate that vertical velocity profiles above the head are quite similar in magnitude and in shape for the two cases. Since  $V^*$  is significantly larger than  $U^*$ , distributions of speed  $Q^*$  in R3 are also very similar for the cases of 'no breathing' and 'continuous exhalation'.

The flow in R1 for 'continuous exhalation' case is a typical example of a buoyant jet in crossflow. The exhalation jet of the present study is deflected upwards by the combined action of buoyancy and momentum of the crossflow rising from the lap of the manikin. The mean velocity of the exhaled air at the exit of nostrils can be assumed to be  $U_j=1.85$  m/s which corresponds to an effective jet diameter of  $D=9 \times 10^{-3}$  m for the prescribed flow rate of exhalation. The Reynolds number based on  $U_j$  and  $D$  is 1100 nominally. The mean value of the vertical velocity in R1 for 'no breathing' case is 0.16 m/s. Therefore, the jet-to-crossflow velocity ratio in this case is approximately 11.6. For a nonbuoyant jet, Özcan and Larsen (2001) report that the jet trajectory, which is defined as the streamline originating from the center of the jet at the exit plane, is coincident with the zero vorticity line around the jet exit. Figures 3 to 5 show that the zero vorticity lines in R3 are located to the left of the dividing streamlines and the zero vorticity line in R1 intersects the dividing streamline in the same manner as it intersects the jet trajectory away from the jet exit for a nonbuoyant jet (Özcan and Larsen, 2001). It may be noted that trajectory of the jets leaving the nostrils in this study do not lie in the plane of symmetry. It is interesting to note that the zero vorticity lines are approximately normal to the speed contours.

Figure 6 gives contour plots of the normalized  $z$ -vorticity  $\zeta_z^* = \partial U^*/\partial y^* - \partial V^*/\partial x^*$ . Parts (a) and (b) present data in R3 for the 'no breathing' case and in R1 for the 'continuous exhalation' case, respectively. Relative uncertainty in  $\zeta_z^*$  is estimated as 15 %. It is important to note that  $\zeta_z^*$  is the only nonzero component of the vorticity vector in the plane of symmetry. Figure 6 (a) shows that vorticity in the boundary layer flow rising from the back of the manikin and vorticity in the plume rising from the front have opposite signs. General levels of vorticity in R3 are not significantly different for the 'no breathing' and 'continuous exhalation' cases. Thus, the magnitude of vorticity in R1 is significantly larger than that of in R3 for the 'continuous exhalation' case.

## 4. Conclusions

Mean velocity data measured around the head of a real-life size seated thermal manikin in the plane of symmetry are presented two cases of 'no breathing' and 'continuous exhalation through nose'. Results of the study are presented in color graphics which describe salient features of the flow field. Main results may be summarized as follows:

1) ( $U$ ,  $V$ ) mean velocity fields of the 'no breathing' and 'continuous exhalation' cases are significantly different not only in the breathing zone (R1) but to a lesser extent also above the breathing zone (R2). Continuous exhalation eliminates the large negative  $U$  region observed in R3 for 'no breathing' case.

2) General levels of speed, vertical velocity and vorticity above the head (in R3) are approximately equal for the 'no breathing' and 'continuous exhalation' cases.

### *Acknowledgements*

The first author acknowledges his sabbatical leave from the Technical University of Istanbul as well as receipt of a grant in scope of the NATO Science Fellowship Programme by the Scientific and Technical Research Council of Turkey and also the financial support of the International Centre for



Indoor Environment and Energy, Department of Mechanical Engineering at the Technical University of Denmark. Fruitful discussions with Professor Poul Scheel Larsen are gratefully acknowledged. Thanks are also due to Jan Holsoe for his assistance in PIV measurements.

### *References*

- Åstrand, P. O. and Rodahl, K., Textbook of work physiology, (1970), McGraw-Hill, New York, USA.
- Chong, M. S. and Perry, A. E., A general classification of three-dimensional flow fields, *Phys. Fluids A*, 2 (1990), 765-773.
- Fanger, P. O., Thermal Comfort, (1970), Danish Technical Press, Copenhagen, Denmark.
- Fiedorowicz, J., Boundary layer of air on a nude man (manikin) caused by free convection heat exchange, (1972), Thermal Insulation Laboratory, Technical University of Denmark, Lyngby, Denmark.
- Homma H. and Yakima, M., Examination of free convection around occupant's body caused by its metabolic heat, *ASHRAE Trans.*, 93 (1987), 104-124.
- Melikov, A. and Zhou, G., Air movement at the neck of the human body, *Proc. of INDOOR AIR 96*, (Naogya, Japan), (1996), 209-214.
- Melikov, A., Kaczmarczyk, J. and Cygan, L., Indoor air quality assessment by a "breathing" thermal manikin, *Proc. of ROOMVENT 2000*, (Reading, UK), (2000).
- Murakami, S., Kato, S. and Zeng, J., Flow and temperature fields around human body with various room air distribution: CFD study on computational thermal manikin (Part1), *ASHRAE Transactions*, 103 (1997), 3-15.
- Özcan, O. and Larsen, P. S., An experimental study of a turbulent jet in crossflow by using LDA, Report MEK-FM 2001-02, (2001), Department of Mechanical Engineering, Technical University of Denmark, Lyngby, Denmark.
- Özcan, O., Meyer K. E. and Melikov, A., Turbulent and stationary convective flow field around the head of a human, *Proc. Of Fourth Int. Symp. on Turbulence, Heat and Mass Transfer*, (Antalya, Turkey), (2003).
- Tobak, M. and Peake, D. J., Topology of three-dimensional separated flows, *Ann. Rev. Fluid Mech.*, 14 (1982), 61-85.

### *Author Profile*



Oktay Özcan: He received his Ph.D. in Mechanical Engineering in 1983 from the University of California at Berkeley, USA. He worked at the NASA-Ames Research Center, USA as an NRC Research Associate between 1982-83 and 1988-90. He was a visiting scientist at the Technical University of Denmark from 1999 to 2001. He has taught at the Technical University of Istanbul between 1984-2002. He has been working at Yıldız Technical University as a professor since 2002. His major research interest is Experimental Fluid Mechanics.



Knud Erik Meyer: He worked two years in a consultant engineering company specialized in heat pumps. He received his Ph.D. degree from the Technical University of Denmark in 1994 on a study of heat transfer in tube bundles involving both experiments and CFD calculations. He is now an associate professor in experimental fluid mechanics. Present research interests are optical flow measurements (LDA, PIV, LIF) and a number of industrial flow applications.



Arsen K. Melikov: Has received his Ph.D. degree in the field of turbulent flows from the Technical University in Sofia. He has performed research and teaching in several countries. At present he is an associate professor in indoor environment, heating ventilation and air conditioning. He has been principle and co-principle investigator of 30 research projects sponsored by government and private organizations from Denmark, Bulgaria, Russia, Ukraine, USA, Japan, Germany, Sweden, Kuwait, Portugal and the European Community.